Title
Controlled release of NELL-1 protein from chitosan/hydroxyapatite-modified TCP particles

Journal
International Journal of Pharmaceutics, 511(1)

ISSN
0378-5173

Authors
Zhang, Yulong
Dong, Rui
Park, Yujin
et al.

Publication Date
2016-09-01

DOI
10.1016/j.ijpharm.2016.06.050

Peer reviewed

HHS Public Access

Author manuscript

Int J Pharm. Author manuscript; available in PMC 2019 August 22.

Published in final edited form as:

Int J Pharm. 2016 September 10; 511(1): 79–89. doi:10.1016/j.ijpharm.2016.06.050.

Controlled release of NELL-1 protein from chitosan/hydroxyapatite-modified TCP particles

Yulong Zhang[a], **Rui Dong**[b], **Yujin Park**[a], **Marc Bohner**[c], **Xinli Zhang**[d], **Kang Ting**[d,e], **Chia Soo**[d,e], **Benjamin M. Wu**[a,d,e,*]

[a]Department of Bioengineering, Department of Materials Science and Engineering, and Division of Advanced Prosthodontics, University of California, Los Angeles, Los Angeles, CA 90095, USA [b]Beijing Institute of Dental Research, School of Stomatology, Capital Medical University, Beijing, 100050, PR China [c]RMS Foundation, Bischmattstr. 12, CH-2544 Bettlach, Switzerland [d]Weintraub Center for Reconstructive Biotechnology, and Dental and Craniofacial Research Institute, School of Dentistry, University of California, Los Angeles, Los Angeles, CA 90095, USA [e]Department of Orthopaedic Surgery, University of California, Los Angeles, Los Angeles, CA 90095, USA

Abstract

NEL-like molecule-1 (NELL-1) is a novel osteogenic protein that showing high specificity to osteochondral cells. It was widely used in bone regeneration research by loading onto carriers such as tricalcium phosphate (TCP) particles. However, there has been little research on protein controlled release from this material and its potential application. In this study, TCP was first modified with a hydroxyapatite coating followed by a chitosan coating to prepare chitosan/hydroxyapatite-coated TCP particles (Chi/HA-TCP). The preparation was characterized by SEM, EDX, FTIR, XRD, FM and Zeta potential measurements. The NELL-1 loaded Chi/HA-TCP particles and the release kinetics were investigated *in vitro*. It was observed that the Chi/HA-TCP particles prepared with the 0.3% (wt/wt) chitosan solution were able to successfully control the release of NELL-1 and maintain a slow, steady release for up to 28 days. Furthermore, more than 78% of the loaded protein's bioactivity was preserved in Chi/HA-TCP particles over the period of the investigation, which was significantly higher than that of the protein released from hydroxyapatite coated TCP (HA-TCP) particles. Collectively, this study suggests that the osteogenic protein NELL-1 showed a sustained release pattern after being encapsulated into the modified Chi/HA-TCP particles, and the NELL-1 integrated composite of Chi/HA-TCP showed a potential to function as a protein delivery carrier and as an improved bone matrix for use in bone regeneration research.

*Corresponding author. Department of Bioengineering, Henry Samueli School of Engineering and Applied Sciences, University of California, Los Angeles, 5121 Engineering V, Los Angeles, CA 90095, USA, benwu@ucla.edu (B.M. Wu).

Conflict of interest

Drs. Wu, Ting, Soo, and Zhang are co-founders of Bone Biologics, Inc., which sublicenses NELL-1 related patents from the UC Regents.

Graphical abstract

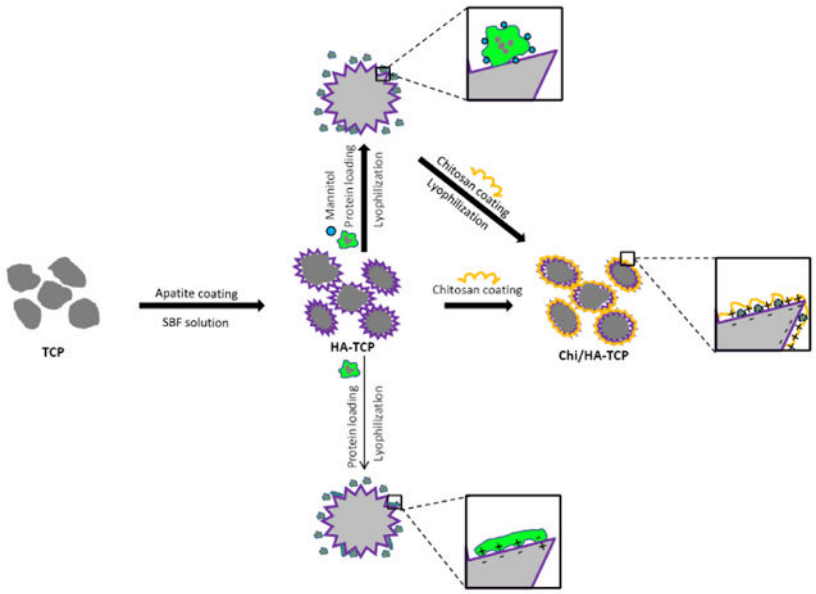

Keywords

NELL-1; Chitosan; hydroxyapatite; TCP; Release kinetics; Bioactivity

1. Introduction:

Nel-like molecule-1 (NELL-1) is a novel osteogenic protein highly expressed in neural tissue. The NELL-1 gene was first isolated and characterized in craniosynostosis patients and was found up-regulated in prematurely fusing sutures (Ting et al., 1999; Zhang et al., 2010).It is directly regulated by Cbfa1/Runx2, thus the downstream regulation made NELL-1 take effect at late stages of osteoblastic differentiation (Aghaloo et al., 2006). NELL-1 is highly specific to osteochondral lineage as a secreted protein. The downstream of Cbfa1/Runx2 and specificity to bone formation made NELL-1 have smaller side effects than BMP-2, the widely used osteogenic protein in clinic. Furthermore, NELL-1 cannot initiate ectopic bone formation in muscle. Therefore, NELL-1 is a promising alternative drug for BMP-2 in osteoinductive therapies. In molecular structure, NELL-1 protein contains 810-amino acid with molecular weight up to 90 KDa before N-glycosylation and oligomerization. The secreted rat NELL-1 is a phosphorylated homotrimeric oligomer with molecular weight over 400 KDa (Kuroda and Tanizawa, 1999).

An ideal bone implant usually consists of growth factors and osteogenic cells. Beside NELL-1, many growth factors such as BMPs, NELL-1, IGFs and TGFβs (Davidson et al., 2015; Linkhart et al., 1996; Mohamad and Khater, 2015; Ting et al., 1999) were also widely used, and osteogenic cells usually includes pluripotential cells and stem cells (de Peppo et al., 2013; Meinel et al., 2004). This kind of composite has been widely used by researchers for skeletal reconstruction, and has always been a key factor in the successful repair or

reconstruction of critical size bone defects (Arner and Santrock, 2014; Babiker, 2013; Bauer and Muschler, 2000; Oryan et al., 2014). Although the autograft is considered to be the gold standard for clinical bone graft operations, it is limited by low obtainable quantities and potential for morbidity during procurement. The advantages of synthetic materials are that they can closely resemble the composition of natural bone, have no risks of immunogenic rejection and disease transmission to the host, and can form a strong bond with the host bone.

As synthetic bone material, Tricalcium phosphate (β-TCP) granules have been widely used as osteoconductive matrices in bone tissue engineering due to their biocompatibility, osteoconductivity and bioactivity *in vivo* (Dong et al., 2002; Walsh et al., 2008; Wiltfang et al., 2003). They are easy to handle and can be molded to fit various kinds of defects, and will not initiate a sustained inflammatory reaction because they can be digested by macrophages and osteoclasts (Lu et al., 2002; von Doernberg et al., 2006). Furthermore, the TCP particles give a negative charged surface in water (Gbureck et al., 2002), which has a nonspecific electrostatic attraction to protein molecules (Gilbert et al., 2000; Raghunathan et al., 2006). This property makes them appropriate as a carrier for protein drug delivery (Abarrategi et al., 2008; Guicheux et al., 1997; Matsumoto et al., 2004; Xie et al., 2010). The loaded growth factors are necessary for TCP bone graft due to the limited osteoinductive ability for TCP material alone. NELL-1 protein has two calcium-binding EGF domains in structure predicted by SMART software, which can specifically bind to the calcium ion on the surface of TCP. Therefore, TCP was usually used as NELL-1 carrier for *in vitro* and *in vivo* application. Previous researches reported that NELL-1 loaded TCP implant enhanced the bone regeneration in various bone defects (Aghaloo et al., 2006; Li et al., 2010). Although the new bone formation was observed, the carrier could be improved by controlling the NELL-1 release and get a long-term release kinetics from the TCP particles. The TCP particles as a drug carrier have a limited loading capacity and the release kinetics of protein from the particles are difficult to control, which can lead to burst or incomplete release (Guicheux et al., 1997; Xue et al., 2009; Ziegler et al., 2002). Since the growth factors released from the scaffold can affect cell migration and proliferation over an extended period of time, the ideal bone graft material is one that allows for a sustained release of the growth factor. The resulting release kinetics play an important role in successful bone regeneration (Zhao et al., 2013). Therefore, finding an optimal way to integrate the biomaterial with NELL-1 is crucial for the development of a smart material, so that it can support the cell adherence and differentiation, control the growth factor release, or even respond to physiological changes in the body (Matassi et al., 2011; Simmons et al., 2004). The aim of this study is to modify β-TCP to make it appropriate as a carrier for NELL-1, so as to enhance its osteoinductive ability of the matrix.

In our current study, the TCP particles were first coated with flake-like hydroxyapatite (HA) in order to make their surface structures more porous and increase the specific surface area, which can significantly improve the protein loading capacity. Then the protein loaded hydroxyapatite-coated TCP (HA-TCP) particles were further modified by coating a chitosan layer in order to control the protein release kinetics. The chitosan has excellent filmogenic property (Muzzarelli et al., 1986), and it can form a strong coating layer on negatively

charged HA surfaces by electrostatic interaction due to its positively charged nature in solution.

The materials and growth factor (NELL-1) in this carrier are not simply mixed, but being integrated together with the hydroxyapatite and chitosan using layer-by-layer method to form a composite (shown as Fig. 1). The special structure of chitosan/hydroxyapatite-coated TCP particles (Chi/HA-TCP) can get sustained NELL-1 release pattern, which is beneficial for osteogenic cells stimulation and improving bone regeneration. The developed carrier could maximize the therapeutic effect after application. The effect of the TCP modification on protein bioactivity and release kinetics was also investigated in this study.

2. Materials and Methods

2.1 Materials:

TCP granules (0.7-1.4 mm, RMS Foundation, Switzerland), Chitosan (Mw 400,000, 85% deacetylated, Sigma), NELL-1 (Aragen Biosciences, CA), Fluorescein isothiocyanate (FITC) kit (Sigma-Aldrich, St. Louis, MO); PBS (phosphate-buffered saline, 50 mM, pH 7.4, Thermo Fisher Scientific, MA). Mannitol, Sucrose, Trehalose, Arginine, and anhydrous ethanol- all analytical grade and used as received from Sigma-Aldrich (St. Louis, MO).

2.2 TCP particle preparation

The TCP particles were prepared by grinding TCP granules (0.7-1.4 mm) into small particles, then using sieves to separate them into different particle sizes. The particles that passed through a #60 sieve (250 μm) and were retained on a #100 sieve (149 μm) were used in this study.

2.3 Hydroxyapatite-coated TCP particle (HA-TCP) preparation

Simulated body fluid solutions (5x SBF1, 5x SBF2) were prepared just before the coating process according to a previously reported protocol (Chou et al., 2004). To begin the coating process, the TCP particles were subjected to glow discharge argon plasma etching for 3 min, then incubated in 5x SBF1 solution for 24 h at 37 °C, rinsed gently with distilled water, followed by incubation in 5x SBF2 for another 48 h at 37 °C, and then washed 3 times with distilled water. Finally, the washed particles were subjected to lyophilization for 24 h. The obtained particles were coated with a layer of biomimetic hydroxyapatite.

2.4 Chitosan/Hydroxyapatite-coated TCP particle (Chi/HA-TCP) preparation

The Chi/HA-TCP particles were prepared by mixing 200 μl of chitosan solution (0.1%, 0.3% or 0.6% chitosan in 50 mM acetic acid solution) with 200 mg of HA-TCP particles. After 0.1 N NaOH was added to adjust the pH value to neutral, the mixture was gently shaken in order to mix them thoroughly. Afterward, the samples were connected to a vacuum system (0.2 Torr) for 2 min to remove the gas in the HA pores and help the chitosan solution penetrate into the pores. Finally, the Chi-HA TCP particles were frozen at −80 °C and lyophilized for 24 h. NELL-1 protein was pre-loaded onto the HA-TCP particles when preparing protein loaded Chi/HA-TCP particles according to the procedure described in section 2.11.1.

2.5 Scanning electron microscope (SEM) characterization

The surface morphology of the TCP, HA-TCP and Chi/HA-TCP particles was observed by SEM (Nova SEM 230, FEI Co., Hillsboro, OR) equipped with EDX (energy-dispersive X-ray spectrometer) for localized chemical analysis. The particles were spread onto carbon conductive adhesive tape, mounted on aluminum stubs, and then observed by SEM under a low vacuum detector. The EDX analysis was conducted at the same time to obtain the elemental composition of the sample surfaces.

2.6 Attenuated total reflection-Fourier transform infrared spectroscopy (ATR-FTIR) characterization

FTIR spectroscopy was performed to analyze the TCP particle surface. Each of the samples (HA-TCP, Chitosan, and Chi/HA-TCP particles) was placed onto the diamond ATR window of an Avatar 360 Thermo Nicolet spectrometer and scanned over the range of 500-4000 cm $^{-1}$ with a resolution of 4 cm^{-1} in transmission mode. The baselines of the spectra were corrected and normalized using OMNIC program (ThermoScientific software for FTIR data collection and analysis).

2.7 X -ray diffraction (XRD) characterization

The crystal structure of the prepared particles (HA-TCP, Chitosan, and Chi/HA-TCP particles) were examined with X-ray diffraction (XRD, D1 system, Bede Inc., UK) using CuKα radiation. The voltage and current settings of the machine is 40 kV and 30 mA respectively. The powders were scanned at a speed of 0.5 °/min, and the XRD diagrams were recorded in the interval between 20° to 45°.

2.8 Fluorescent microscopy (FM) characterization

2.8.1 Fluorescein isothiocyanate (FITC)-chitosan preparation—The FITC-chitosan was prepared according to a method reported by Sarmento et al. (Sarmento et al., 2011). Briefly, 7.5 mL of 1.0% chitosan solution (50 mM acetic acid solution) was treated with an excess amount of FITC (0.25 mg, dissolved in 200 μl of anhydrous ethanol) under constant magnetic stirring (300 RPM), and the reaction was allowed to continue for 3 h. The FITC-labeled chitosan polymer was precipitated by adding 10 mL of 0.1 M NaOH to the reaction mixture. The precipitated FITC-chitosan polymer was then centrifuged at 5 KRPM for 5 min and washed repeatedly with a mixture of ethanol/water (70/30) until the supernatant was free of FITC (confirmed using fluorescence intensity measurements). The obtained FITC-chitosan was then lyophilized and stored in a freezer.

2.8.2 Fluorescent microscopy (FM) observation—FM characterization was performed to confirm the homogeneity of the chitosan coating on the HA-TCP particles. FITC-chitosan was coated on the HA-TCP particles according to the procedure described in section 2.4. The lyophilized particles were then placed onto a glass slide and mounted on the stage of a fluorescence microscope (Leica DM IRB inverted fluorescence microscope, German), and images were acquired using a Zeiss 10x objective lens.

2.9 Zeta potential of the Chitosan/Hydroxyapatite-TCP particles

The surface charge of the Chi/HA-TCP particles was determined by measuring the zeta potentials of the particles in 10^{-3} M KCL solution using a Zetasizer Nano-ZS90 (Malvern Instruments, Westborough, MA). The testing was performed according to a method reported in the literature (Thielbeer et al., 2011). Briefly, 0.2 mg of the Chi/HA-TCP particles was mixed with 10 mL of 10^{-3} M KCL solution adjusted with sodium chloride to a conductivity of 50 μS/cm, and was magnetically stirred at 200 RPM for 5 min. One mL of the suspension was then transferred into a zeta potential cuvette for measurement at 25 °C.

2.10 Excipient screening for NELL-1 loading process

The small molecular excipients: trehalose (Tre), sucrose (Suc), mannitol (Man), and arginine (Arg), which are widely used as protein protectors (Bedu-Addo, 2004; Izutsu et al., 2009; Lu and Pikal, 2004), were investigated to measure their ability of enhancing the release of NELL-1 from HA-TCP particles. In this study, FITC-labeled NELL-1 (FITC-NELL-1) was prepared as previous method (Zhang et al., 2014) and loaded onto HA-TCP particles by lyophilization method. Briefly, 20 μL of excipient and NELL-1 solution (containing 5 μg of FITC-NELL-1 and 5% of excipient) was added to 20 mg of HA-TCP particles. They were incubated together for 1 h at 4 °C. The FITC-NELL-1 loaded particles were frozen and lyophilized overnight. FITC-NELL-1 loaded HA-TCP particles without any excipients were prepared at the same time and used as control. The prepared samples were added into 1.0 mL of PBS to perform release experiments under gentle shaking at 4 °C. The release samples were collected at 1, 2, 3, 5, 7, 10, and 14 days, and replenished with fresh PBS after each collection. The protein concentration of the released samples was determined using a plate reader (Infinite F200, Tecan Group Ltd.) at the excitation and emission wavelength of 490 and 515 nm, respectively. All release experiments were performed in triplicate.

2.11 Release kinetics of Chi/HA-TCP particles

2.11.1 Preparation of NELL-1-loaded Chi/HA-TCP particles—To further control the release kinetics of NELL-1 from the particles, a chitosan layer was coated on to the NELL-1 loaded HA-TCP particles. Briefly, the TCP particles were first coated with plate-like hydroxyapatite, and then 40 μL of NELL-1 solution (containing 10 μg NELL-1, 5% mannitol) was lyophilized onto 40 mg of HA-TCP particles. The obtained particles were added to 40 μL of 0.3% chitosan solution in order to prepare the NELL-1-loaded Chi/HA-TCP particles according to the procedure described in section 2.4.

2.11.2 Release kinetics—The release kinetic pattern of the NELL-1-loaded Chi/HA-TCP particles was measured in this study. The FITC labeled NELL-1 was used to determine the protein concentration by plate reader. Briefly, the protein loaded Chi/HA-TCP particles was first immersed in 1 mL of release medium (PBS with 10% FBS and 1% Pent/Strep) at 4 °C under gentle shaking. Then the release samples were collected at pre-determined time points (1, 2, 3, 5, 7, 10, 14, 21, and 28 days), and NELL-1 concentration was determined as described in section 2.10.

2.12 Bioactivity of released NELL-1

The bioactivity of the NELL-1 released from the particles was determined by measuring its ability to increase the expression of alkaline phosphatase (ALP) in mouse calvarial osteoblast cells. The cells were isolated from calvaria of 3-5 day old mice (strain C57BL/6) and cultured in growth medium (DMEM containing 10% FBS, 50 U/mL penicillin, and 50 ng/mL streptomycin) (Zhang et al., 2014). The release samples from 0-3 days, 4-10 days, and 11-28 days were combined together and used for a cell-based bioactivity assay. The release samples were diluted to 300 ng/mL with osteogenic medium (DMEM containing 10% FBS, 10 mM β-glycerophosphate, 50 μg/mL L(+)-ascorbic acid, 50 U/mL penicillin, and 50 ng/mL streptomycin) prior to testing. The release samples from Chi/HA-TCP particles without NELL-1 were used as a negative control, and fresh NELL-1 solution with the same concentration (300 ng/mL) was used as a positive control.

The ALP testing was performed as reported in the literature (Zhang et al., 2014). Briefly, the mouse calvarial osteoblast cells were seeded on 24-well plates and starved for 16 h at 37 °C. Then the culture medium was replaced by the osteogenic medium containing either NELL-1 release samples or standard NELL-1. The cells were cultured at 37 °C in 5% CO_2 humidified incubators, and the osteogenic medium was changed every two days. After 9 days of incubation, the cells were solubilized in 200 μL of lysis buffer (0.2 % NP-40, 1 mM magnesium chloride) at 4 °C for 15 min. The cell supernatant was separated and reacted with ALP substrate buffer for 15 min at 37 °C. After stopping the reaction with NaOH, the absorbance of the mixture was measured at 405 nm using a plate reader (Infinite F200, Tecan Group Ltd.). The ALP activity was normalized to total cellular protein measured by Bradford protein assay. All measurements were performed in triplicate.

3. Results

3.1 SEM and EDX characterization

The particles were prepared by crushing β-TCP granules and collecting the particles that passed through a #60 sieve and retained on a #100 sieve. Based on the size histogram (Fig. 2G), the mean size of the obtained β-TCP particles was 190.7±33.4 μm.

The morphology and size of the particles were observed by SEM and shown in Fig.2. The β-TCP particles exhibited an irregular shape under SEM, and after being coated with hydroxyapatite, the flake-like apatite layer on the particle surfaces and the pores between the flakes were observed (Fig. 2C, 2D). A cross-section image of the apatite layer is shown in Fig. 2H, which highlights the thickness of the apatite layer, estimated at 4.67±0.88 μm. After being coated with chitosan, however, the chitosan film filled the pores of the apatite layer and covered the surface of the ATCP particles (Fig. 2E, 2F). Further characterization with EDX showed the chemical composition of the different kinds of particles (Fig. 2B, 2D, 2F). The TCP, HA-TCP and Chi/HA-TCP particles showed high-intensity peaks for calcium (3.69, 4.00 keV) and phosphorus (2.01 keV). The Ca/P atomic ratios for β-TCP, HA-TCP and Chi/HA-TCP were 1.50±0.07, 1.45±0.09, and 1.44±0.20, respectively. The Ca/P atomic ratio for hydroxyapatite was less than the standard value (1.67), but was consistent with values previously reported in the literature (Chou et al., 2004).

3.2 FTIR characterization

FTIR was used to characterize the particles before and after being coated with chitosan. The baselines of the spectra were corrected and normalized, and the results are shown in Fig. 3A comparison of the spectra revealed that the characteristic peaks of chitosan could be observed in the spectrum of the Chi/HA-TCP particles. For example, the peak corresponding to the stretching of intermolecular hydrogen bonding of v_{OH} and v_{NH} in chitosan was centered at 3446 cm^{-1}, and the Amide I band corresponding to $v_{C=O}$ vibration of acetyl groups in chitosan was observed around 1650 cm^{-1}. The Amide III band was observed at 1332 cm^{-1} due to a combination of NH deformation and v_{CN} stretching vibration, and the band resulting from v_{C-O} was observed at 1089 cm^{-1}. The analysis of the FTIR spectra of the samples therefore confirmed the presence of chitosan on the Chi/HA-TCP particles in contrast with the uncoated HA-TCP particles.

3.3 XRD characterization

The XRD patterns of different particles were shown in Fig.4. There is no peaks in the range of 22-45° for Chitosan sample, and HA-TCP and Chi/HA-TCP particles showed similar peaks in the patterns. The peaks at 23.3, 25.9, 29.3, and 32.2 came from the diffraction planes (211), (002), (210), and (300) of HA crystallites, respectively, which confirmed the formation of HA on TCP particles. After being coated with chitosan, the crystallization of the HA still existed. Thus the crystalline characteristic peaks of HA were not changed significantly by chitosan coating.

3.4 FM characterization

FITC-chitosan was prepared and the calculated FITC content of the synthesized FITC-chitosan was 2.6%. HA-TCP particles were first coated with FITC-chitosan, and the obtained Chi/HA-TCP particles were observed under FM. It can be seen in Fig. 5 that the irregular particles were scattered on the glass slide and there is no observed agglomerates. Moreover, the homogeneous distribution of green fluorescent color on the particles suggested that the chitosan was uniformly spread and formed a polymer layer on the HA-TCP particles.

3.5 Zeta potential characterization

The zeta potential of the particles was measured in order to determine the change of surface charge before and after coating. Fig. 6 presents the surface charge measured using different particles. It can be seen that the zeta potential of uncoated TCP and HA-TCP are −18 ± 2 and −28 ± 2 mV, respectively, but after being coated with chitosan, the surface charge of particles increased up to +22 ± 1 mV with a chitosan concentration of 0.3%. Increasing the concentration beyond 0.3% did not lead to a further increase in the zeta potential.

3.6 Excipient screening for NELL-1 release

In order to control NELL-1 release by preserving its conformation and changing its interaction with the HA-TCP surface, various excipients (trehalose, sucrose, mannitol, and arginine) were added to the formulation of the NELL-1 solution used to load the HA-TCP particles. These excipients are known to be able to preserve the conformation of a protein by

a preferential interaction mechanism during adsorption and lyophilization (Bedu-Addo, 2004). The release profiles shown in Fig. 7 illustrated the difference in release rates between the various formulations. For all formulations, there was a burst release of less than 5% in the first day, followed by a slow release profile with varying release rates depending on the excipients used, and all samples containing excipients had a higher release rate than the control prepared without excipients. The formulation using the mannitol exhibited a sustained release profile and had the highest release rate (1.23 %/d). Furthermore, its NELL-1 release amount was 21.25 ± 1.06 % at day 14, which was statistically higher than that of other excipient formulations. Mannitol was therefore chosen as the excipient to adjust the release of NELL-1 from HA-TCP particles.

3.7 Kinetics of NELL-1 release from Chi/HA-TCP particles

The release kinetics of NELL-1 from Chi/HA-TCP particles was determined by loading Chi/HA-TCP particles with FITC-labeled NELL-1 protein. The release profile of the loaded Chi/HA-TCP particles is presented in Fig. 8, which shows a sustained release pattern in the entire experiment period ($Y=1.9574X+33.073$, $R^2=0.9849$, from day 3 to day 28), and about 80% of the NELL-1 was released at 28 days. It was found that the 0.3% chitosan layer and 0.6% chitosan layer resulted in similar release profiles, and there was no statistically significant difference between them. Although 0.1% chitosan layer showed a sustained release, it showed a much higher burst release amount (up to 53±6%) compared to the 0.3% and 0.6%. However, for the formulations without the chitosan layer, 69±6% of the NELL-1 was released by the first day, and there was almost no protein release by day 7. These results suggest that the Chi/HA-TCP carrier (0.3% chitosan) successfully controlled the NELL-1 release.

3.8 Bioactivity of released NELL-1 in vitro

In order to test the activity of the released NELL-1 protein, the release samples were first diluted to a concentration of 300 ng/mL NELL-1 using cell culture medium. The bioactivity of NELL-1 from the release samples was compared with the bioactivity of fresh NELL-1, the blank release medium was used as negative control, and the results were shown in Fig. 9. The activity of the NELL-1 released from Chi/HA-TCP from 0-3 days was 92± 5% when compared to the bioactivity of fresh NELL-1 solution, and it was significantly higher than the corresponding 82± 6% activity of NELL-1 released from the HA-TCP particles without mannitol and chitosan layer. In fact, analysis using SPSS software shows that throughout the entire release period, the bioactivity of NELL-1 released from Chi/HA-TCP particles was statistically higher than that of NELL-1 released from unmodified HA-TCP particles. Therefore, compared to the HA-TCP particles without chitosan and mannitol, the special structure of the Chi/HA-TCP particles make it possible to significantly preserve the bioactivity of NELL-1.

4. Discussion

NELL-1 protein has a large molecular weight of 400 KDa and complicated conformation in structure (Zhang et al., 2010), which make it fragile in activity and remarkably sensitive to denaturation and activity loss during preparation and storage. Loading proteins onto carriers

is widely used method in bone regeneration system. The thermal stability of the encapsulated protein is generally enhanced based on the theory of macromolecular crowding and molecular confinement (Eggers and Valentine, 2001). The protein encapsulated in the carrier also can prevent denaturation caused by enzyme, temperature, pH value change during application *in vivo*. In this study, we designed a new kind of TCP material, Chi/HA-TCP particles, which can encapsulate NELL-1 protein into the particles. The NELL-1 stability can be preserved in the system and give a sustained release pattern. The procedure and mechanism of chitosan coating on HA-TCP particles are illustrated in Fig. 1. First, the TCP particles were coated with hydroxyapatite (HA), which can assist the formation of strong bonds between new bone and the TCP particles, because it can help the deposition of biological microapatite perpendicular to the TCP surface, as well as the association of the TCP particles with collagen fiber in new bone tissue (Zhou and Lee, 2011). The coating can thus facilitate bone ingrowth into the particles and promote osseointegration. Then the HA-TCP particles were coated with a chitosan layer. The chitosan was chosen due to its excellent filmogenic properties (Muzzarelli et al., 1986), and it can form a homogeneous layer on the irregular TCP particles. Moreover, chitosan is positively charged in solution due to the numerous amine groups in its linear polysaccharide structure (Di Martino et al., 2005), which can specifically bind to the negatively charged surface of the hydroxyapatite-coated TCP particles through electrostatic interactions. Most importantly, the chitosan layer which is tightly bound to the HA-TCP particles can be used to control the release of protein loaded on the HA-TCP particles. Besides, the resulting film can provide a biocompatible and bioresorbable substrate for different types of cell cultures (Di Martino et al., 2005), making it a suitable biodegradable biopolymer for covering complex surfaces. Furthermore, the mechanical strength of the HA-TCP particles will not be attenuated by the surface modification since there is no change in the bulk of the TCP particles.

FITC-chitosan was used to investigate the chitosan coating on the HA-TCP particles. Fluorescent image (Fig. 5) revealed that the chitosan was completely and homogeneously coated on the HA-TCP particle surfaces. The particles after coating were easily separated into single particles. SEM images supported that the HA-TCP surface was completely covered by the chitosan polymer and showed that the pores between the HA flakes had been filled as well (Fig. 2E, 2F). Further EDX analysis revealed that the calcium to phosphate atomic ratio (Ca/P) of the prepared hydroxyapatite was smaller than the standard ratio (1.67) of pure hydroxyapatite, which suggested that the apatite used for TCP particle coating had a calcium deficient structure (Chou et al., 2004). This could result in a negatively charged surface that would be beneficial for protein adsorption and loading, which was later confirmed by zeta potential measurement.

Because the characteristic nitrogen peaks of chitosan were difficult to detect on the EDX spectra for the Chi/HA-TCP particles, FTIR measurement was performed to confirm the chitosan nature of the coating. Fig. 3 showed a small peak at around 1650 cm^{-1} corresponding to the $v_{c=o}$ vibration of the amide I band in chitosan, as well as at 1332 cm^{-1} due to a combination of NH deformation and the v_{CN} stretching vibration. These results suggest the existence of chitosan layer on the HA-TCP particle surface. Therefore, the Chi/HA-TCP particles were successfully prepared. The effect of Chitosan coating on HA structure was investigated by XRD measurement. The characteristic peaks of HA were still

observed in Chi/HA-TCP particles (Fig. 4), and there is no significant change in location and intensity, which indicated that the chitosan coating did not change the HA microstructure.

When developing a chitosan coating formulation for the HA-TCP particles, one of the issues that need to be addressed was that excess chitosan can encapsulate particles to form a bulky matrix. It was therefore important to limit the chitosan amount in the formulation so that there was enough polymer to completely cover the HA-TCP particle surfaces, but not excess to cause matrix formation. In FM analysis, separately scattered particles were observed for the particles coated with the 0.3% (wt/wt) chitosan formulation (Fig. 5). In order to further investigate the effect of the chitosan coating on the particle surface, the surface charge of the Chi/HA-TCP particles was measured by Zetasizer Nano-ZS90, and the results were shown in Fig. 6. After being coated with hydroxyapatite, the zeta potential of the β-TCP particles decreased from −18± 2 mV to −27± 2 mV. However, after chitosan coating, the zeta potential of the particles changed from a negative to a positive number. The zeta potential of the Chi/HA-TCP particles initially increased with chitosan concentration, but after reaching a maximum at the concentration of 0.3%, the zeta potential plateaued and did not increase further with chitosan concentration. This indicates that the 200 μl of the 0.3% chitosan solution was enough to completely cover the surface of 200 mg of HA-TCP particles, which is consistent with the result of FM characterization.

Usually the NELL-1 protein was directly loaded onto the HA-TCP particles by lyophilization (James et al., 2012; Li et al., 2010). There was a chance that significant conformational changes occurred when the protein encountered the solid surfaces of the particles, which could lead to denaturing and incomplete release of adsorbed proteins from the particles in PBS medium (Crotts et al., 1997; Dong et al., 2007; Gray, 2004). This is caused by the strong bonds between solid particle surface and unfolded protein. Coulomb forces formed during loading process between the charged groups (Ca^{2+}, PO_4^{3-}) of hydroxyapatite and the exposed functional groups ($-OH$, $-NH_2$, $-COO^-$, etc.) of the unfolded protein (Fig. 1). In our pilot study, about 80% of the NELL-1 protein loaded on HA-TCP particles was left unreleased in PBS medium even after a period of 1 month (data not shown). This type of incomplete release can be solved by employing release medium containing serum or surfactant, which can neutralize the electrostatic interaction between protein and HA surface (Lee et al., 2007), and lead to a complete release. Appropriate excipients can be added to preserve the original conformation and bioactivity of the protein during the loading process in lyophilization (Bedu-Addo, 2004), so that the protein can be adsorbed onto the apatite surface without undergoing a significant change in conformation. Upon interaction with the release medium, the protein can easily be released from the anchoring sites and went into the surrounding medium.

We investigated several small molecular protectants that are widely used in lyophilization formulations, trehalose (Tre), sucrose (Suc), mannitol (Man) and arginine (Arg), and investigated their effect on the release kinetics of NELL-1 from apatite particles. The release profiles shown in Fig.7 illustrated the difference between the various excipients. The data were analyzed with linear regression (Tab. 1), and the release profiles showed a significant difference on slopes ($P<0.0001$). The formulation containing mannitol had the highest NELL-1 release rate. The results indicate that mannitol was the most effective excipient in

forming a protective shield around the NELL-1 molecules and preventing its structure to unfold. Therefore, mannitol was added to the formulation during NELL-1 loading onto the Chi/HA-TCP particles.

The next step was to test the release kinetics of the designed carrier. It is known that the release medium can significantly affect the release patterns of drug carriers (Faisant et al., 2006; Lee et al., 2007). In a routine release experiment, a simple dissolution media such as PBS (50 mM, pH7.4) is preferred because of its low cost and ease of preparation. PBS was therefore selected as the release medium for the excipient screening study. However, for the Chi/HA-TCP particles, a more complicated medium (PBS containing 10% FBS and 1% Pent/Strep) was used to simulate the composition of the biological fluids *in vivo* at the site where the carrier will be implanted, so as to get a more accurate representation of the release kinetics. The Chi/HA-TCP particles demonstrated a sustained and controlled release pattern compared to the HA-TCP particles prepared without chitosan. The ability of the Chi/HA-TCP particles to control the NELL-1 release was attributed to the chitosan layer working as a diffusion barrier. Without the control of the chitosan layer, the uncoated HA-TCP particles showed a standard two-phase release pattern, often described as a brief initial rapid or burst release phase followed by an extended gradual slow release phase. This is consistent with historical reports on protein release from apatite carriers (Downes et al., 1991; Guicheux et al., 1998; Laffargue et al., 2000). It is necessary for the initial release to provide enough of the protein immediately after implantation to have a therapeutic effect, but serious side effects may occur if too much of the protein is released. Therefore, it is important to minimize the extent of the initial protein burst release. The electrostatic interaction is not enough to control the protein release in the complicated release medium, the particles were further modified by coating a layer of chitosan. After modification, an improved release pattern was observed, and it showed a significantly decreased initial release, as well as a NELL-1 release rate that remains constant of 2.02%/d for over 28 days (Fig. 8).The porous surface of the HA-TCP particles would act as a NELL-1 deposit and the additional chitosan layer would function as a release barrier for the protein. The NELL-1 protein released from the HA-TCP surface could diffuse through the chitosan layer into the release medium. The positively charged chitosan chains of the layer could also interact with negatively charged regions of the NELL-1 protein and further impeded its release from the particles.

The protein released from carrier is not necessarily bioactive. The protein was easily adhered to the glass surface of the release container or the surface of HA plates, which will lead to the loss of activity. Therefore, we examined whether the released NELL-1 could still facilitate the differentiation of mouse calvarial osteoblast cells *in vitro*. In this study, the activity of the released NELL-1 was evaluated at different time ranges. Fig. 9 and Tab. 2 showed the bioactivities of the released NELL-1 from different carriers. Bioactivity loss of NELL-1 was observed for both HA-TCP and Chi/HA-TCP carriers during release, but more than 78% of the bioactivity (compared to that of fresh NELL-1 protein) was retained over the 28-day release experiment for the Chi/HA-TCP particles, whereas only 66 ± 4% was retained for the HA-TCP particles. The bioactivity of HA-TCP and Chi/HA-TCP showed a significant difference after statistical analysis by one-way ANOVA. These results suggest that the Chi/HA-TCP carrier not only successfully controls NELL-1 release, but also preserves its bioactivity.

This study demonstrated that the designed Chi/HA-TCP particles have beneficial features as a novel protein carrier, including sustained protein release and preservation of protein bioactivity. It could be a promising composite for bone defect regeneration, and our future studies will aim to explore its application in animals.

5. Conclusion

The findings of this study suggest that the release kinetics of the novel osteogenic protein NELL-1 was significantly improved by the designed Chi/HA-TCP particles, and a slow, steady release pattern of NELL-1 up to 28 days was observed. Furthermore, the formulation preserved the bioactivity of the protein when compared to native HA-TCP particles. The modified Chi/HA-TCP particles have the ability to encapsulate growth factors and to maintain sustained release kinetics, which brings the integrated composite closer to natural bone tissue. The design of this new carrier lays down the framework for further studies of its applications as a promising material for use in bone regeneration research.

Acknowledgments

This work was supported by the CIRM Early Translational II Research Award TR2-01821 and NIH/NIAMS 1 R01 AR060213-01. The authors thank Dr. Mark S. Goorsky, Chao li for their help in XRD characterization.

References:

Abarrategi A, Moreno-Vicente C, Ramos V, Aranaz I, Sanz Casado JV, López-Lacomba JL, 2008 Improvement of porous β-TCP scaffolds with rhBMP-2 chitosan carrier film for bone tissue application. Tissue Engineering Part A 14, 1305–1319. [PubMed: 18491953]

Aghaloo T, Cowan CM, Chou Y-F, Zhang X, Lee H, Miao S, Hong N, Kuroda S.i., Wu B, Ting K, 2006 Nell-1-induced bone regeneration in calvarial defects. The American journal of pathology 169, 903–915. [PubMed: 16936265]

Arner JW, Santrock RD, 2014 A historical review of common bone graft materials in foot and ankle surgery. Foot & ankle specialist 7, 143–151. [PubMed: 24425807]

Babiker H, 2013 Bone graft materials in fixation of orthopaedic implants in sheep. Danish medical journal 60, B4680. [PubMed: 23809979]

Bauer TW, Muschler GF, 2000 Bone graft materials. An overview of the basic science. Clinical orthopaedics and related research, 10–27.

Bedu-Addo FK, 2004 Understanding lyophilization formulation development. Pharmaceutical Technology 20, 10–19.

Chou Y-F, Chiou W-A, Xu Y, Dunn JC, Wu BM, 2004 The effect of pH on the structural evolution of accelerated biomimetic apatite. Biomaterials 25, 5323–5331. [PubMed: 15110483]

Crotts G, Sah H, Park TG, 1997 Adsorption determines in-vitro protein release rate from biodegradable microspheres: quantitative analysis of surface area during degradation. Journal of Controlled Release 47, 101–111.

Davidson EB, van Caam A, Vitters E, Bennink M, Thijssen E, van den Berg W, Koenders M, van Lent P, van de Loo F, van der Kraan P, 2015 A4. 6 TGF-β is a potent inducer of nerve growth factor in articular cartilage via the ALK5-SMAD2/3 pathway. Potential role in OA related pain? Annals of the Rheumatic Diseases 74, A38–A38.

de Peppo GM, Marcos-Campos I, Kahler DJ, Alsalman D, Shang L, Vunjak-Novakovic G, Marolt D, 2013 Engineering bone tissue substitutes from human induced pluripotent stem cells. Proceedings of the National Academy of Sciences 110, 8680–8685.

Di Martino A, Sittinger M, Risbud MV, 2005 Chitosan: a versatile biopolymer for orthopaedic tissue-engineering. Biomaterials 26, 5983–5990. [PubMed: 15894370]

Dong J, Uemura T, Shirasaki Y, Tateishi T, 2002 Promotion of bone formation using highly pure porous β-TCP combined with bone marrow-derived osteoprogenitor cells. Biomaterials 23, 4493–4502. [PubMed: 12322969]

Dong X, Wang Q, Wu T, Pan H, 2007 Understanding adsorption-desorption dynamics of BMP-2 on hydroxyapatite (001) surface. Biophysical journal 93, 750–759. [PubMed: 17617550]

Downes S, Di Silvio L, Klein C, Kayser M, 1991 Growth-hormone loaded bioactive ceramics. Journal of Materials Science: Materials in Medicine 2, 176–180.

Eggers DK, Valentine JS, 2001 Molecular confinement influences protein structure and enhances thermal protein stability. Protein Science 10, 250–261. [PubMed: 11266611]

Faisant N, Akiki J, Siepmann F, Benoit J, Siepmann J, 2006 Effects of the type of release medium on drug release from PLGA-based microparticles: experiment and theory. International journal of pharmaceutics 314, 189–197. [PubMed: 16510257]

Gbureck U, Probst J, Thull R, 2002 Surface properties of calcium phosphate particles for self setting bone cements. Biomolecular engineering 19, 51–55. [PubMed: 12202161]

Gilbert M, Shaw WJ, Long JR, Nelson K, Drobny GP, Giachelli CM, Stayton PS, 2000 Chimeric peptides of statherin and osteopontin that bind hydroxyapatite and mediate cell adhesion. Journal of Biological Chemistry 275, 16213–16218. [PubMed: 10748043]

Gray JJ, 2004 The interaction of proteins with solid surfaces. Current opinion in structural biology 14, 110–115. [PubMed: 15102457]

Guicheux J, Gauthier O, Aguado E, Heymann D, Pilet P, Couillaud S, Faivre A, Daculsi G, 1998 Growth hormone-loaded macroporous calcium phosphate ceramic: In vitro biopharmaceutical characterization and preliminary in vivo study. Journal of biomedical materials research 40, 560–566. [PubMed: 9599032]

Guicheux J, Grimandi G, Trécant M, Faivre A, Takahashi S, Daculsi G, 1997 Apatite as carrier for growth hormone: in vitro characterization of loading and release. Journal of biomedical materials research 34, 165–170. [PubMed: 9029295]

Izutsu K.-i., Kadoya S, Yomota C, Kawanishi T, Yonemochi E, Terada K, 2009 Freeze-drying of proteins in glass solids formed by basic amino acids and dicarboxylic acids. Chemical and Pharmaceutical Bulletin 57, 43–48. [PubMed: 19122314]

James AW, Zara JN, Zhang X, Askarinam A, Goyal R, Chiang M, Yuan W, Chang L, Corselli M, Shen J, 2012 Perivascular stem cells: a prospectively purified mesenchymal stem cell population for bone tissue engineering. Stem cells translational medicine 1, 510–519. [PubMed: 23197855]

Kuroda S.i., Tanizawa K, 1999 Involvement of epidermal growth factor-like domain of NELL proteins in the novel protein–protein interaction with protein kinase C. Biochemical and biophysical research communications 265, 752–757. [PubMed: 10600492]

Laffargue P, Fialdes P, Frayssinet P, Rtaimate M, Hildebrand HF, Marchandise X, 2000 Adsorption and release of insulin-like growth factor-I on porous tricalcium phosphate implant. Journal of biomedical materials research 49, 415–421. [PubMed: 10602075]

Lee M, Chen TT, Iruela-Arispe ML, Wu BM, Dunn JC, 2007 Modulation of protein delivery from modular polymer scaffolds. Biomaterials 28, 1862–1870. [PubMed: 17184836]

Li W, Lee M, Whang J, Siu RK, Zhang X, Liu C, Wu BM, Wang JC, Ting K, Soo C, 2010 Delivery of lyophilized Nell-1 in a rat spinal fusion model. Tissue Engineering Part A 16, 2861–2870. [PubMed: 20528102]

Linkhart TA, Mohan S, Baylink DJ, 1996 Growth factors for bone growth and repair: IGF, TGFβ and BMP. Bone 19, S1–S12.

Lu J, Descamps M, Dejou J, Koubi G, Hardouin P, Lemaitre J, Proust JP, 2002 The biodegradation mechanism of calcium phosphate biomaterials in bone. Journal of biomedical materials research 63, 408–412. [PubMed: 12115748]

Lu X, Pikal MJ, 2004 Freeze-Drying of Mannitol-Trehalose-Sodium Chloride-Based Formulations: The Impact of Annealing on Dry Layer Resistance to Mass Transfer and Cake Structure. Pharmaceutical development and technology 9, 85–95. [PubMed: 15000469]

Matassi F, Nistri L, Paez DC, Innocenti M, 2011 New biomaterials for bone regeneration. Clinical cases in mineral and bone metabolism 8, 21–24. [PubMed: 22461799]

Matsumoto T, Okazaki M, Inoue M, Yamaguchi S, Kusunose T, Toyonaga T, Hamada Y, Takahashi J, 2004 Hydroxyapatite particles as a controlled release carrier of protein. Biomaterials 25, 3807–3812. [PubMed: 15020156]

Meinel L, Karageorgiou V, Fajardo R, Snyder B, Shinde-Patil V, Zichner L, Kaplan D, Langer R, Vunjak-Novakovic G, 2004 Bone tissue engineering using human mesenchymal stem cells: effects of scaffold material and medium flow. Annals of biomedical engineering 32, 112–122. [PubMed: 14964727]

Mohamad MI, Khater MS, 2015 Evaluation of insulin like growth factor-1 (IGF-1) level and its impact on muscle and bone mineral density in frail elderly male. Archives of gerontology and geriatrics 60, 124–127. [PubMed: 25240725]

Muzzarelli R, Aiba S, Fujiwara Y, Hideshima T, Hwang C, Kakizaki M, Izume M, Minoura N, Rha C, Shouij T, 1986 Filmogenic properties of chitin/chitosan, Chitin in nature and technology. Springer, pp. 389–402.

Oryan A, Alidadi S, Moshiri A, Maffulli N, 2014 Bone regenerative medicine: classic options, novel strategies, and future directions. Journal of orthopaedic surgery and research 9, 18. [PubMed: 24628910]

Raghunathan V, Gibson JM, Goobes G, Popham JM, Louie EA, Stayton PS, Drobny GP, 2006 Homonuclear and heteronuclear NMR studies of a statherin fragment bound to hydroxyapatite crystals. The Journal of Physical Chemistry B 110, 9324–9332. [PubMed: 16671751]

Sarmento B, Mazzaglia D, Bonferoni MC, Neto AP, do Céu Monteiro M, Seabra V, 2011 Effect of chitosan coating in overcoming the phagocytosis of insulin loaded solid lipid nanoparticles by mononuclear phagocyte system. Carbohydrate Polymers 84, 919–925.

Simmons CA, Alsberg E, Hsiong S, Kim WJ, Mooney DJ, 2004 Dual growth factor delivery and controlled scaffold degradation enhance in vivo bone formation by transplanted bone marrow stromal cells. Bone 35, 562–569. [PubMed: 15268909]

Thielbeer F, Donaldson K, Bradley M, 2011 Zeta potential mediated reaction monitoring on nano and microparticles. Bioconjugate chemistry 22, 144–150. [PubMed: 21244000]

Ting K, Vastardis H, Mulliken JB, Soo C, Tieu A, Do H, Kwong E, Bertolami CN, Kawamoto H, Kuroda S.i., 1999 Human NELL-1 Expressed in Unilateral Coronal Synostosis. Journal of Bone and Mineral Research 14, 80–89. [PubMed: 9893069]

von Doernberg M-C, von Rechenberg B, Bohner M, Grünenfelder S, van Lenthe GH, Müller R, Gasser B, Mathys R, Baroud G, Auer J, 2006 In vivo behavior of calcium phosphate scaffolds with four different pore sizes. Biomaterials 27, 5186–5198. [PubMed: 16790273]

Walsh WR, Vizesi F, Michael D, Auld J, Langdown A, Oliver R, Yu Y, Irie H, Bruce W, 2008 β-TCP bone graft substitutes in a bilateral rabbit tibial defect model. Biomaterials 29, 266–271. [PubMed: 18029011]

Wiltfang J, Schlegel KA, Schultze-Mosgau S, Nkenke E, Zimmermann R, Kessler P, 2003 Sinus floor augmentation with β-tricalciumphosphate (β-TCP): does platelet-rich plasma promote its osseous integration and degradation? Clinical oral implants research 14, 213–218. [PubMed: 12656882]

Xie G, Sun J, Zhong G, Liu C, Wei J, 2010 Hydroxyapatite nanoparticles as a controlled-release carrier of BMP-2: absorption and release kinetics in vitro. Journal of Materials Science: Materials in Medicine 21, 1875–1880. [PubMed: 20300953]

Xue W, Bandyopadhyay A, Bose S, 2009 Polycaprolactone coated porous tricalcium phosphate scaffolds for controlled release of protein for tissue engineering. Journal of Biomedical Materials Research Part B: Applied Biomaterials 91, 831–838.

Zhang X, Zara J, Siu R, Ting K, Soo C, 2010 The role of NELL-1, a growth factor associated with craniosynostosis, in promoting bone regeneration. Journal of dental research 89, 865–878. [PubMed: 20647499]

Zhang Y, Velasco O, Zhang X, Ting K, Soo C, Wu BM, 2014 Bioactivity and circulation time of PEGylated NELL-1 in mice and the potential for osteoporosis therapy. Biomaterials 35, 6614–6621. [PubMed: 24818884]

Zhao J, Wang S, Bao J, Sun X, Zhang X, Zhang X, Ye D, Wei J, Liu C, Jiang X, 2013 Trehalose maintains bioactivity and promotes sustained release of BMP-2 from lyophilized CDHA scaffolds for enhanced osteogenesis in vitro and in vivo. PloS one 8, e54645. [PubMed: 23359400]

Zhou H, Lee J, 2011 Nanoscale hydroxyapatite particles for bone tissue engineering. Acta biomaterialia 7, 2769–2781. [PubMed: 21440094]

Ziegler J, Mayr-Wohlfart U, Kessler S, Breitig D, Günther KP, 2002 Adsorption and release properties of growth factors from biodegradable implants. Journal of biomedical materials research 59, 422–428. [PubMed: 11774299]

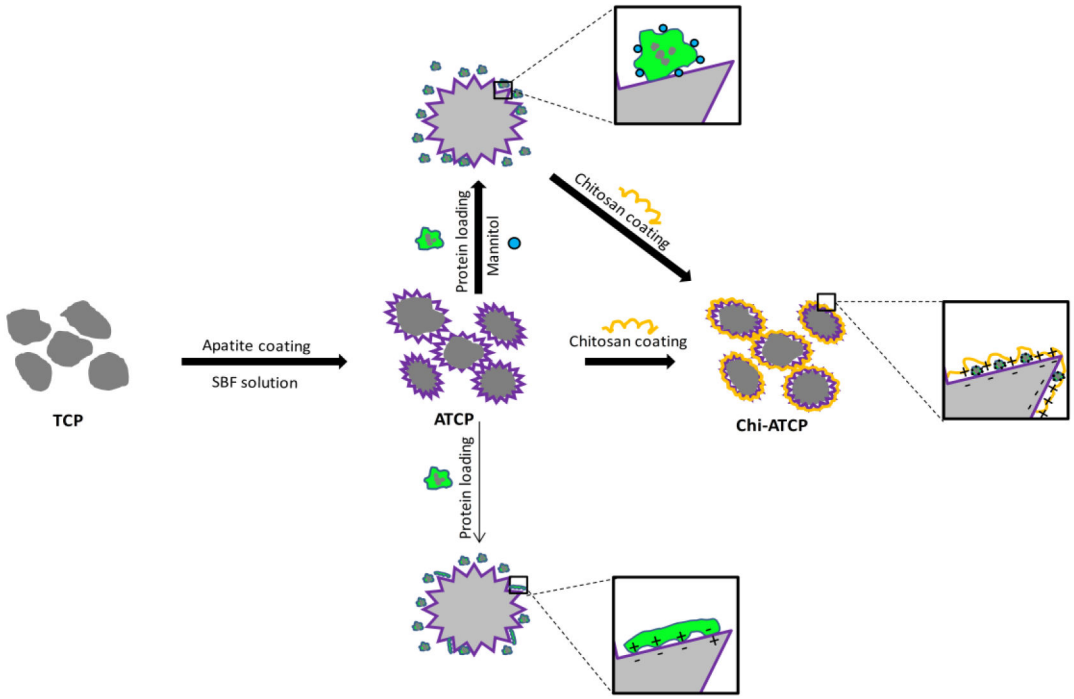

Fig.1.

Schematic graph of Chi/HA-TCP preparation and the mechanism of protein or chitosan interacting with HA-TCP particles. TCP particles were first coated with hydroxyapatite by incubating in SBF solutions, and then coated with chitosan to prepare Chi/HA-TCP particles. The NELL-1 protein could be loaded onto HA-TCP particles by lyophilization. Mannitol was included in the protein formulation to preserve protein conformation and to prevent its denaturation and incomplete release caused by electrostatic interactions between the protein and particle surfaces.

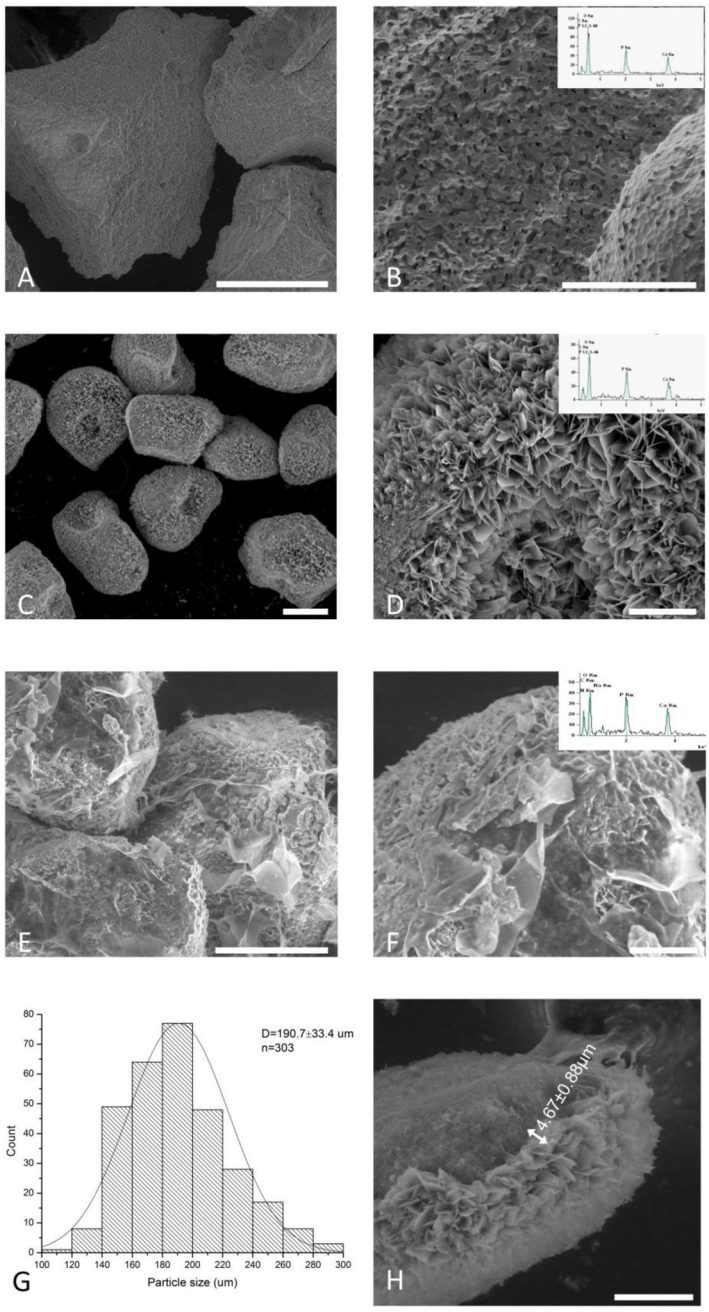

Fig.2.

SEM images of β-TCP particles (A,B), HA-TCP particles (C,D), and Chi/HA-TCP particles (E,F) at different magnifications. The corresponding EDX analysis of the particles is presented in the top right corner of the figures (B,D,F). (G) Particle size histogram of the sieved β-TCP particles. (H) Thickness of the hydroxyapatite layer was 4.67±0.88 μm. The flake-like apatite and pores between the flakes were clearly visible (D). After chitosan coating, chitosan film was filled in the pores of the apatite layer (F). The left scale bar is 100 μm, and the right one is 30 μm.

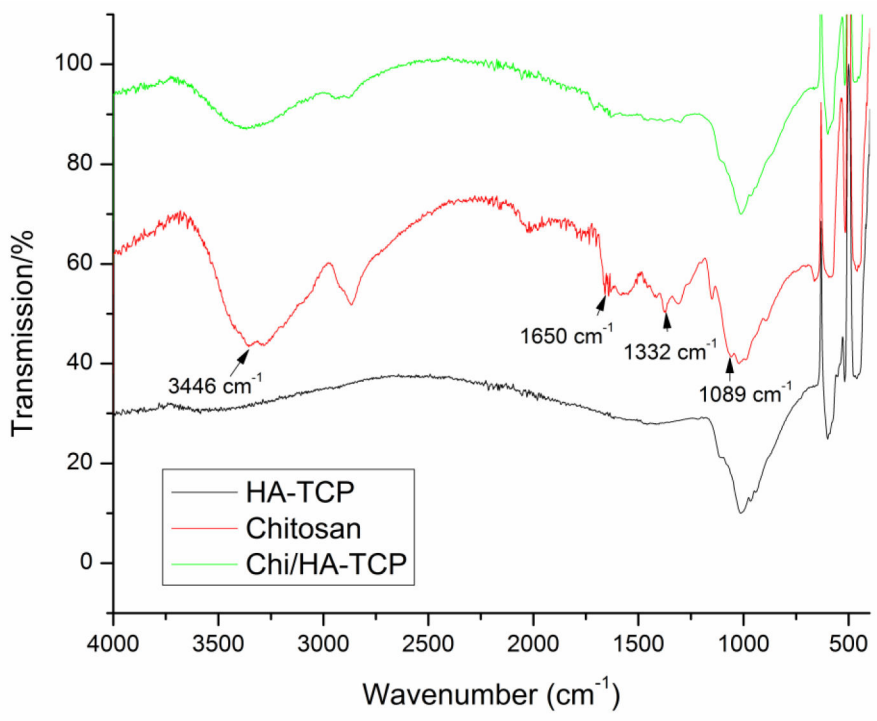

Fig.3.

ATR-FTIR spectra of HA-TCP, Chitosan and Chi/HA-TCP particles. The characteristic peaks of chitosan were labeled as: intermolecular hydrogen bond stretching (ν_{OH}, ν_{NH}) centered at 3446 cm^{-1}, Amide I band corresponding to $\nu_{C=O}$ vibration in chitosan's acetyl groups at 1650 cm^{-1}, Amide III band at 1332 cm^{-1} due to combination of NH deformation and ν_{CN} stretching. These peaks were also visible in the Chi/HA-TCP spectrum, confirming the presence of chitosan on the particles.

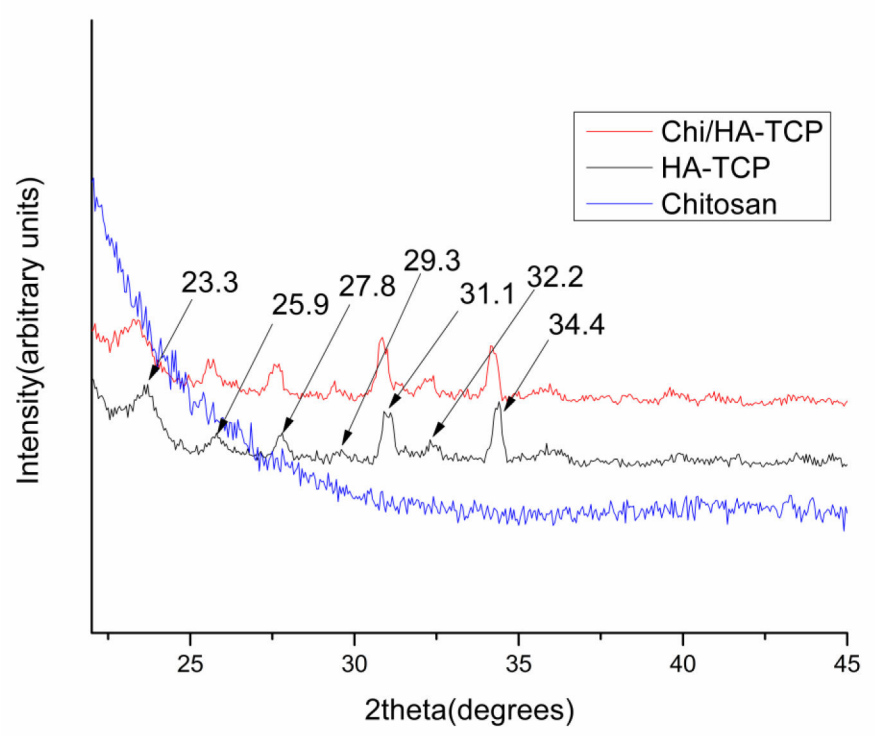

Fig. 4.

XRD pattern of HA-TCP, Chitosan and Chi/HA-TCP particles. After being coated with chitosan, the crystallization of the HA-TCP did not change.

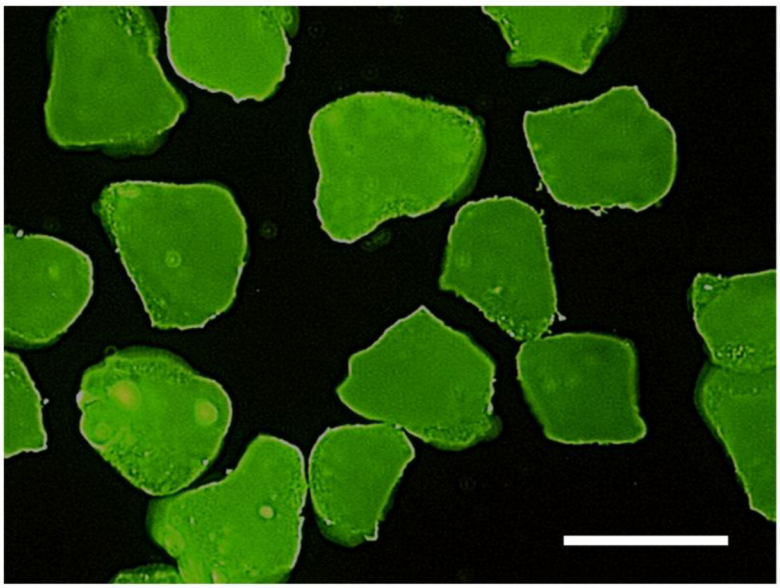

Fig.5.

FM image of Chi/HA-TCP particles using FITC-chitosan at 0.3% (wt/wt) concentration. Separately scattered particles were observed when using 0.3% (wt/wt) chitosan. Scale bar: 200 μm.

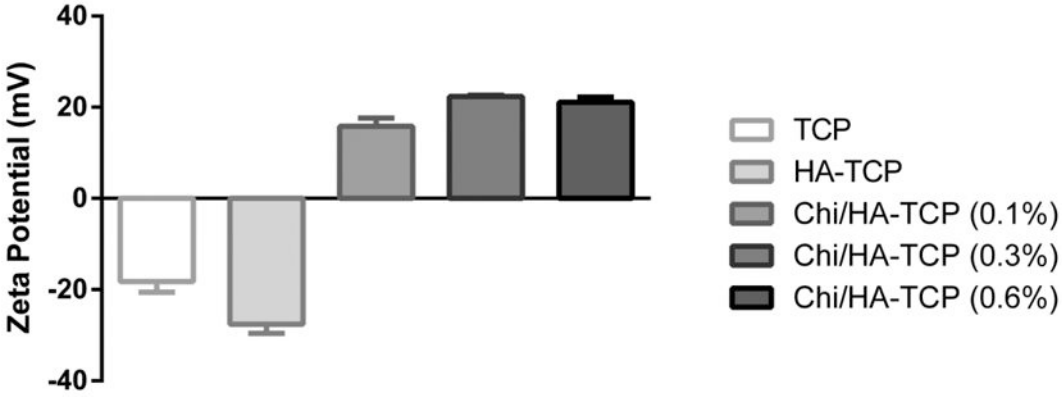

Fig.6.

Zeta potential values of the particles with different coatings. The measured zeta potential values for TCP, HA-TCP, and Chi/HA-TCP (0.3%) were −18±2 mV, −28±2 mV, and +22±1 mV, respectively.

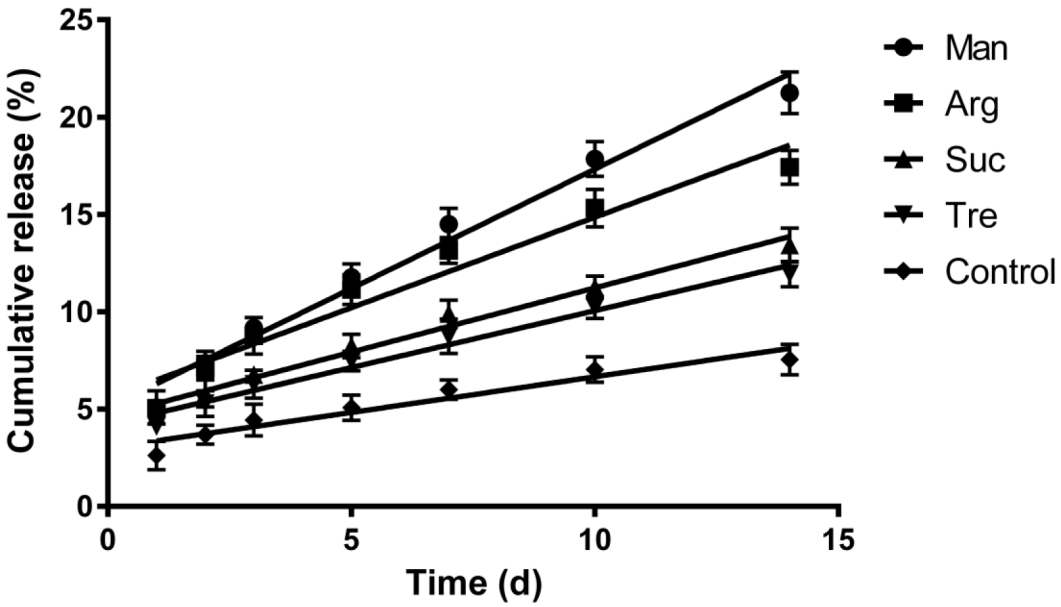

Fig.7.

The effect of different excipients on the NELL-1 release from HA-TCP particles in PBS medium. The data were fitted with linear regression model.

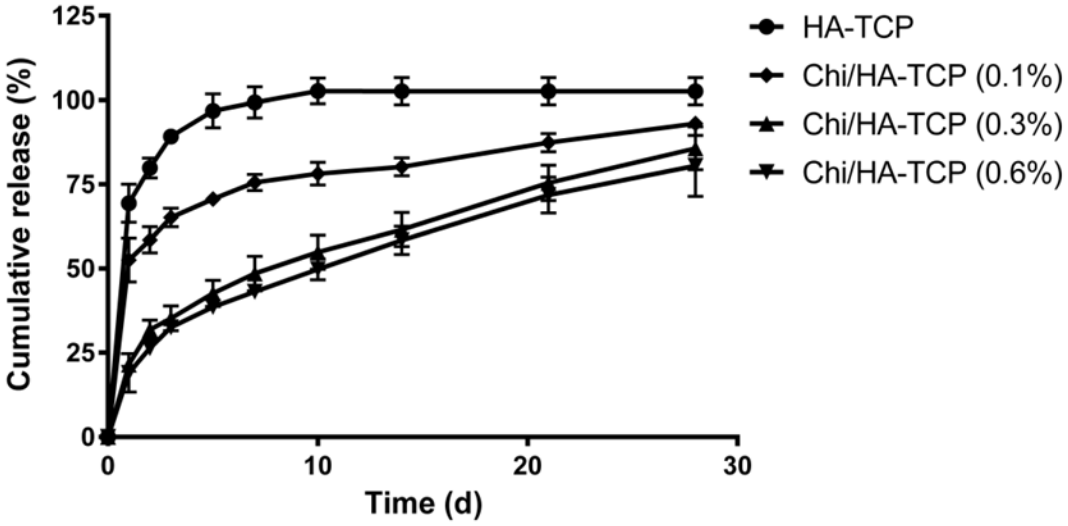

Fig.8.

Comparison of the release profiles for unmodified HA-TCP and Chi/HA-TCP particles (0.1, 0.3, 0.6% Chitosan) in release medium containing 10% FBS and 1% Pent/Strep. HA-TCP particles showed a fast release and 70% of NELL-1 was released on the very first day, but Chi/HA-TCP particles had a controlled and sustained protein release profiles.

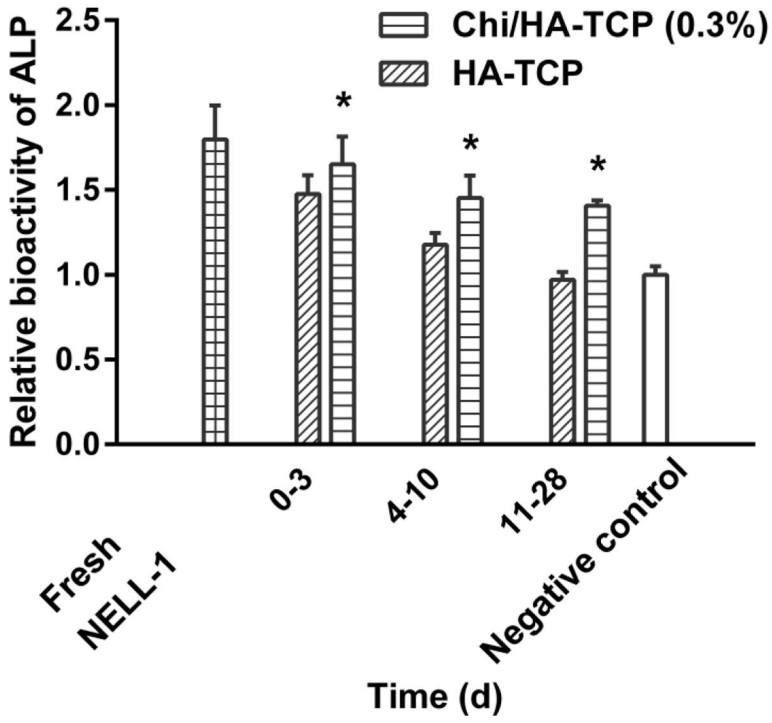

Fig.9.

The bioactivity of released NELL-1 from ATCP and Chi/HA-TCP particles. Bioactivity was measured by testing its ability to increase ALP expression in mouse calvarial osteoblast cells. Chi/HA-TCP particles without NELL-1 were used as a negative control. The bioactivity of NELL-1 released from Chi/HA-TCP was consistently higher than that of NELL-1 released from HA-TCP at all time points.

Tab.1

Analysis of the various release profiles of formulations using different excipients. The data were analyzed by linear regression, and the lines showed a significant difference on slopes. (F=27.0791, P<0.0001)

Excipients	Man	Arg	Suc	Tre	Control
Linear	Y = 1.225*X +	Y = 0.9285*X +	Y = 0.6600*X +	Y = 0.5843*X +	Y = 0.3650*X +
equation	5.075	5.569	4.629	4.214	3.010
Slope	1.225±0.0771	0.9285±0.0946	0.6600±0.0408	0.5843±0.0410	0.3650±0.0462
R^2	0.9806	0.9506	0.9813	0.9760	0.9259

Tab.2

Relative bioactivity (fresh NELL-1 as 100%)

Time	0-3d	4-10d	11-28d
HA-TCP	82±6	66±4	54±3
Chi/HA-TCP	92±5	81±7	78±2